Collisional redistribution in Hg-Kr: Polarization spectrum of the redistributed light

I. M. Bell, C. J. K. Quayle, and K. Burnett
Clarendon Laboratory, Oxford, OX1 3PU, United Kingdom

D. M. Segal
Blackett Laboratory, Imperial College, London SW7 2BZ, United Kingdom
(Received 9 November 1992)

We have measured the alignment of Hg($6\,^3P_1$) atoms following off-resonant excitation of the Hg $6\,^1S_0$–$6\,^3P_1$ transition in the presence of Kr. We present a polarization spectrum for both red and blue wings out to detunings beyond 100 cm^{-1}. This represents a considerable extension to the existing results, which has been made possible by the use of a pump-and-probe excitation scheme. In the experiment a pulsed laser, detuned from the resonance, creates an alignment in the upper state. This is probed by tuning a delayed second laser to a higher transition and monitoring laser-induced fluorescence from the two-step process. The alignment of the asymptotic Hg($6\,^3P_1$) atoms is determined by comparison of the signals obtained for different relative polarizations of the lasers. We discuss the advantages of this method and the relation of the raw data to the polarizations presented. The results are discussed within the context of a simple quasiclassical model of the process.

PACS number(s): 34.50.Rk, 34.20.Mq, 34.30.+h, 32.90.+a

I. INTRODUCTION

Polarization-monitored collisional redistribution experiments previously have been carried out in several metal–rare-gas systems [1-8]. In these experiments, atoms with a resonance at frequency ω_0 are situated in a much higher concentration of rare-gas perturber atoms. Polarized light at a frequency ω_L, near ω_0, then illuminates the mixture. Most experiments have been performed with linearly polarized light in which case the resulting spectrum is observed perpendicularly to the propagation direction of the incident light. In the weak-field limit this spectrum consists of two components: Rayleigh scatter peaked around ω_L and fluorescence peaked on line center. The latter is the collisionally redistributed component due to collisionally assisted excitation followed by spontaneous emission.

The polarization of the emitted light is defined as

$$P=\frac{I_z-I_x}{I_z+I_x}\ , \tag{1}$$

where I_z and I_x are the intensities of the scattered light polarized in the z and x directions, respectively. Here the incident light is assumed to propagate along the y axis with its polarization vector in the z direction. Polarization analysis is usually achieved by rotating the polarization of the incident light and having a fixed analyzer in the detection line. Dispersion of the fluorescence and Rayleigh scatter is accomplished using a monochromator or Fabry-Pérot interferometer.

For a $J=0\rightarrow 1$ transition the Rayleigh scatter is always perfectly polarized, i.e, $P=1$. The polarization of the redistributed component, on the other hand, depends on the dynamics of the collision and is the quantity of interest in these experiments.

The theory of collisional redistribution of radiation has been developed along two lines. In the first, absorption of radiation during collisions is incorporated in a generalized master-equation approach. This was used to show how the information from polarized collisional redistribution experiments complements that available from standard far wing line-shape experiments [9-11]. The other approach is based on dressed atomic collision theory. This technique uses quantum collision theory with extra channels to allow for radiative couplings. It has been developed to exploit the machinery of many-channel molecular scattering theory, both formal and computational, and is well suited to quantitative calculation [12-15].

Interpretation of experimental data in terms of these theoretical approaches is inevitably rather complicated; therefore much use has been made of an intuitive quasiclassical model due to Lewis *et al.* [16]. This model deals with the quasistatic region of the line shape and, in its most basic form, makes four main assumptions. (i) A classical straight-line trajectory is followed throughout the collision. (ii) Excitation occurs at a real Condon point to a specific molecular state, with probability determined by quasistatic line-shape theory. No account is taken of the coherence induced between different molecular states by the excitation process, except in the case of degeneracy. (iii) Adiabatic following of the molecular potentials occurs throughout the collision. (iv) The transition from a molecular to an atomic description occurs discontinuously at a radius R_{dc}, the decoupling radius.

The origin of the depolarization associated with collisional redistribution is obvious within the framework of this model. The molecular orbital created on excitation is "body fixed" and will rotate with the internuclear axis as the collision progresses, until decoupling from it at R_{dc}. If the orbital excited is not invariant under such ro-

tations [i.e., does not have Π^- (1^-) symmetry] it will suffer some reorientation by this process. This reorientation of the orbital means that the subsequent fluorescence from the asymptotic atom will not be polarized in the same direction as the incident light. The average over all orientations of collision frame leads to the observed depolarization of the redistributed light.

Interatomic potentials for the system in question are required as input to any theoretical treatment of collisional redistribution. In addition to its dependence on details of the collision dynamics, the polarization of collisionally redistributed light is also sensitive to the form of the interatomic potentials. The motivation to make measurements on Hg-Kr stems from the wealth of reliable potential data that is available for this system. This comes both from temperature-dependent line-shape measurements [17,18] and measurements on the spectra of Hg-Kr van der Waals molecules formed in a supersonic expansion [19,20]. Results on the Hg-Kr system should therefore allow models of the collision process to be tested directly against experimental data.

The interatomic potentials of Grycuk and co-workers [17,18] for the Hg-Kr system are shown in Fig. 1. Hund's case-(c) coupling applies and the state assignations are $X\,^1 0^+$ for the ground state and $A\,^3 0^+$ and $B\,^3 1^\pm$ for the excited states. The difference potentials are also also shown in this figure.

The Hg-Kr system has been the subject of a previous study by this group [7]. However, due to low signal levels our results were limited to red-wing detunings less than 40 cm^{-1} and two points in the blue wing. Increasing the signal by raising the mercury vapor pressure was not possible due to the associated increase in depolarization due to radiation trapping. The correction for this depolarizing mechanism is difficult to estimate and must be kept as small as possible.

On the basis of the simple quasiclassical model described above one would expect wide range of polarizations to be exhibited in the red wing. At small detunings the excitation occurs predominantly to the B state, while at larger detunings excitation may only occur to the A state (see the difference potential plot in Fig. 1). The 1^- state, as we have already noted, causes no depolarization, so excitation to the $A\,^3 0^+$ state is more depolarizing than excitation to the $B\,^3 1^\pm$ state. The model therefore predicts a switch in the polarization from high values in the near wing to somewhat lower values in the far wing.

Our previous results showed a slight downward trend in polarization as the detuning to the red is increased. The polarizations measured at the highest detunings could be interpreted as the beginnings of a switch to lower polarizations, but this is not conclusive due to the low signal-to-noise levels encountered at these detunings. It was therefore difficult to say whether even the main qualitative prediction of the model (i.e., the red-wing polarization switch) had been confirmed.

The present work is intended to push the existing results further out in to the red wing, so that definite conclusions may be made about the polarization switch. More ambitiously we wish to provide a set of data in both wings which is of adequate precision to allow direct comparisons with fully quantal and semiclassical calculations. The existence of a fully quantum-mechanical coupled-channel calculation for this system [21] is a further motivation for the experiment.

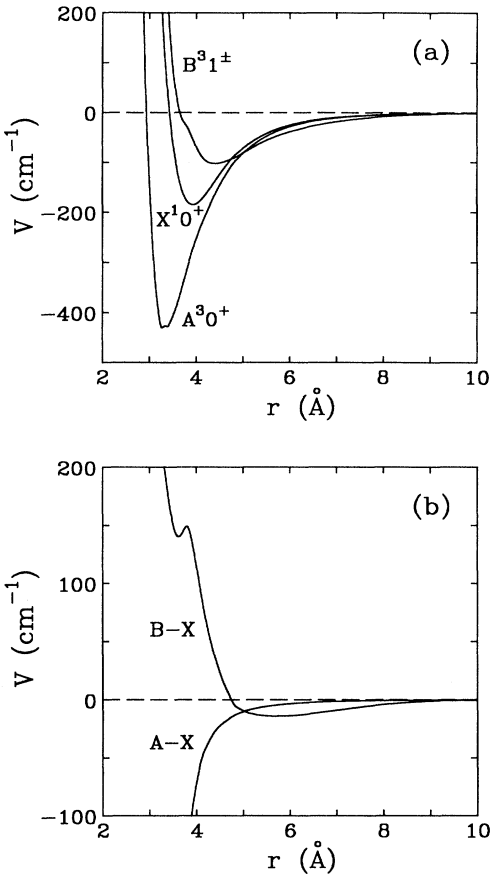

FIG. 1. Hg-Kr interatomic potentials of Grycuk and coworkers. (a) The ground-state $X\,^1 0^+$ potential and excited state $A\,^3 0^+$ and $B\,^3 1^\pm$ potentials are shown, referred to the same asymptote. (b) Difference potentials between ground and excited states.

II. EXPERIMENT

The mercury transitions involved in this experiment are shown in Fig. 2. The uv light is slightly detuned from the 253.7-nm Hg $6\,^1S_0 - 6\,^3P_1$ intercombination line. In the absence of perturbers, excitation of a Hg($6\,^1S_0$) atom cannot occur. The intermediate Hg-Kr collision complex, however, may be excited at internuclear separations localized around the Condon points. After decoupling to atomic states the asymptotic Hg($6\,^3P_1$) atoms suffer excitation by the delayed probe laser, which is tuned to the $6\,^3P_1 - 7\,^3S_1$ transition at 435.8 nm. Laser-induced fluorescence (LIF) on the $7\,^3S_1 - 6\,^3P_2$ transition at 546.1 nm is observed through a mercury green line filter.

The ratio of LIF measured with the laser polarizations parallel to that obtained when they are perpendicular is monitored in this experiment. Measurement of this ratio

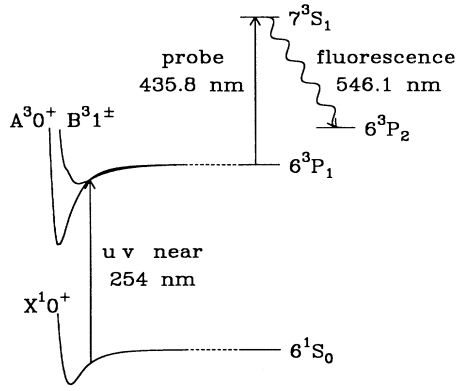

FIG. 2. Excitation scheme for the experiment. The uv laser, detuned from the atomic resonance, can only cause excitation during a collision. After a short delay, a second laser resonant with a higher transition probes the excited state. Total LIF is detected on a third transition. The potential well depths are exaggerated.

allows a value of $\rho_{00}/\rho_{\pm1\pm1}$ ($\rho_{M_JM_J}$ is the M_J state population) to be determined for the asymptotic Hg($6\,^3P_1$) atoms. This involves a fairly lengthy, but straightforward, analysis of the four-level system. Determination of $\rho_{00}/\rho_{\pm1\pm1}$ amounts to a measurement of the atomic alignment. The polarization of the 253.7-nm fluorescence, as defined in Eq. (1), may then be recovered through

$$P=\frac{\rho_{00}-\frac{1}{2}(\rho_{-1-1}+\rho_{+1+1})}{\rho_{00}+\frac{1}{2}(\rho_{-1-1}+\rho_{+1+1})} . \tag{2}$$

This is usually the quantity measured in collisional redistribution experiments and our results are therefore presented in terms of this parameter. With detection orthogonal to the probe laser polarization and to the propagation direction of the lasers we obtain

$$P=\frac{I_\perp-I_\parallel}{I_\perp+I_\parallel/\kappa} . \tag{3}$$

Here $I_\parallel$ and $I_\perp$ are the LIF signals obtained with the polarization directions of the lasers parallel and perpendicular, respectively. We emphasize that the two equivalent experimental expressions for P [Eqs. (1) and (3)] depend on completely different experimental information. It is not surprising, therefore, that there is no direct correspondence between the intensities $I_\parallel, I_\perp$ and I_z, I_x. The parameter κ is slightly dependent upon the detection geometry. With a negligible solid angle of detection we find $\kappa=13$. Its value rises to 13.62 with the finite solid angle of detection ($\pi/16$ sr) employed in this experiment.

The above assumes absence of M_J changing collisions in the $7\,^3S_1$ state after excitation. This should be well satisfied for Hg($7\,^3S_1$)–Kr due to the small alignment destroying collision cross section [22] and the short radiative lifetime ($\sim$10 ns) of this state. It is worth noting that, if upper state collisions were more important, they could have at most a 2% effect on our measured polarizations. This is in the limit where the collisions completely destroy the upper state alignment. It also applies if all of the LIF (i.e., 4π sr) were detected. This demonstrates the lack of sensitivity of our polarization measurements to upper-state collisions. It also shows that the measured polarizations are not critically dependent upon a precise determination of the collection angle.

Such considerations are, of course, bypassed entirely if a $^1S_0$ state is used as the upper state. In this case there is complete independence from the detection direction or upper-state collisions. For mercury however, there is no $^1S_0$ state which is spectrally convenient for the operation of Nd:YAG pumped dyes (where YAG denotes yttrium aluminum garnet). We therefore sacrificed some ease of analysis for experimental convenience in this work.

The arrangement described above has several advantages over direct polarization analysis of the 253.7-nm fluorescence. The most important of these is the greater signal level that may be achieved: the need for a monochromator in the detection line is eliminated and LIF may be collected from a large solid angle. Photon counting, an essential part of the earlier experiments, is no longer required for any detuning at which data were taken.

Other advantages of this system are associated with its minimization of the influence of secondary depolarizing mechanisms. Details of secondary depolarizing mechanisms are given in Sec. III. The first of these advantages is due to the asymptotic Hg($6\,^3P_1$) atom alignment being probed after a time t_d, the laser delay, rather than a time-averaged value being measured. The time t_d may be made small in comparison to the lifetime of the Hg($6\,^3P_1$) state (118 ns). As a result, those depolarizing mechanisms which act on a nanosecond time scale (second collisions, Hanle effect, radiation trapping) will have less effect on the polarization. The second advantage is that the extent of radiation trapping is now determined by the laser-beam waists rather than the size of the experimental cell. This makes it considerably less significant than in a single-step experiment, as was previously noted by Alford *et al.* [6].

A. Experimental details and procedure

The experimental apparatus is shown schematically in Fig. 3. Ultraviolet light close to the Hg 253.7-nm line is produced by frequency doubling the output of a coumarin 500 dye laser in a crystal of β-BaB_2O_4 (BBO). Light resonant on the Hg 435.8-nm transition is obtained from a coumarin 440 dye laser. Both dye lasers are homemade, the oscillators are based on a Littman-type design [23] with intracavity beam expanders. The output from the coumarin 500 oscillator is amplified before doubling. The dye lasers are pumped by the third harmonic of a Nd:YAG laser with a 10-Hz repetition rate. They have bandwidths of around 7 GHz with pulse durations of about 5 ns. The lasers typically produce 5 μJ in the uv and 30 μJ from the coumarin 440 oscillator.

The experimental cell is a four-armed glass cross of total length 20 cm. The arms are circular in cross section with diameter 5.5 cm; three are terminated with quartz windows. Direct laser scatter is reduced by baffling the

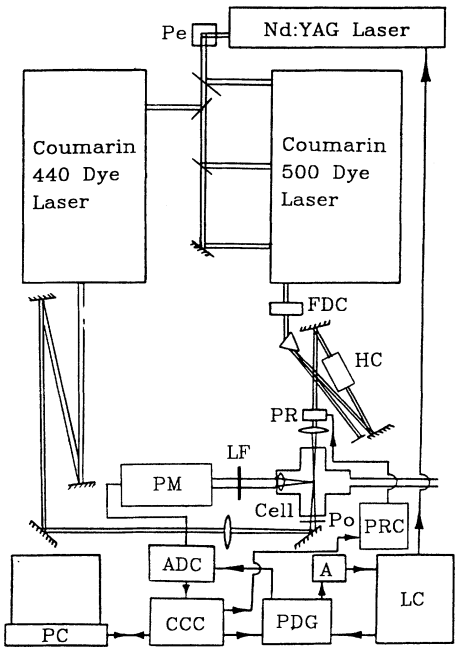

FIG. 3. Schematic representation of the experimental setup. *CCC*, CAMAC crate controller; PDG, pulse delay generator; *A*, trigger pulse amplified; LC, Nd:YAG laser controller and power supply; Pe, periscope; FDC, frequency-doubling crystal; HC, mercury hot cell; PR, polarization rotator: $\lambda/2$ plate; PRC, polarization rotator controller; Po, polarizer; LF, mercury green line filter; PM, photomultiplier; ADC, analog-to-digital converter.

windows on the laser-beam line and blackening the interior surface of the cell.

The laser beams are arranged to counterpropagate in the cell and focused to beam waists of 100 μm. A delay line of about 4 m is introduced so that the light from the probe laser reaches the interaction region after the uv pulse. The uv passes through a heated quartz cell containing mercury before reaching the interaction region. This absorbs any frequency-doubled amplified spontaneous emission on line center, which would otherwise resonantly pump the Hg($6\,^1S_0$) atoms.

On leaving the frequency-doubling crystal the uv is vertically polarized. It passes through a stepper motor driven $\lambda/2$ plate which is rotated through 45° every 50 laser shots. By this method the polarization of the uv entering the cell is made alternately vertical and horizontal. The delayed laser is polarized vertically by passing the beam through a crystal polarizer immediately prior to entering the cell. The crystal polarizer is crossed with the $\lambda/2$ plate (in horizontal orientation) by minimizing the uv passing through both, using a photodiode.

Light from the interaction region is collimated by a 5-cm-diam, $f=10$ cm lens placed inside the cell. It is filtered by a Hg 546.1-nm line filter (10 nm bandpass) before falling on the cathode of a photomultiplier. The output of the photomultiplier is fed directly to an analog-to-digital converter (ADC) acting as a charge integrator. The ADC is gated to reduce laser-off background using a pulse delay generator (PDG). The PDG also provides the trigger for the Nd:YAG pump laser. The experiment is controlled and data collected by a personal computer which is interfaced to the stepper motor driver, PDG and ADC by means of a Transiac CAMAC crate controller.

B. Background and systematics

A background count is observed in the absence of the probe laser. We attribute this to the uv causing the quartz windows to fluoresce at wavelengths that the line filter can pass. The collisionally redistributed signal is expected to fall off as a Lorentzian, i.e., $1/\Delta\omega^2$, in the absence of satellites, while this background remains constant. It is therefore negligible in comparison to the signal at small detunings, but rises to approximately 10% of signal for the largest detunings at which polarizations were measured. This background is monitored and where significant it is subtracted from the data. The largest corrections in the polarization that this procedure produces are of around the same magnitude as the statistical error.

We have measured the polarization that is obtained in this experiment for resonant two photon excitation. For this measurement the lasers are both detuned by 10 cm^{-1} from the one photon resonance, while the two photon resonance is maintained. The delay is removed so that the pulses are temporally coincident. A polarization of $99.90\pm0.14\%$ was measured in this configuration. This sets a lower limit on the polarization of the lasers in the interaction region. However, this almost perfect polarization of the lasers will only be relevant to the experiment if response to the probe laser is linear. If, on the other hand, this laser saturates the transition, small components of intensity orthogonal to the laser polarization direction may become significant. This effect has been investigated experimentally in the delayed configuration by insertion of neutral density filters into the probe beam. We found that with increasing probe laser intensity, the polarization measured at fixed detuning starts to decrease quite soon after linear response of the signal ceases.

For this reason we work with the probe laser intensity inside the linear regime. Commonly this requires the insertion of neutral density filters which pass only 0.25% of the coumarin 440 laser output. This corresponds to a pulse energy of 75 nJ. In this regime the result quoted above for the polarization of the resonant two photon excitation may be used to give an estimate of the likely depression of our measured polarizations due to imperfect polarization of the lasers. We calculate an upper limit to this depression as 0.3% of the measured value. This is small in comparison to the statistical error and no attempt is made to correct the data for this effect.

As the probe laser frequency is moved away from resonance a reduction in polarization is observed along with the expected decrease in signal. This indicates the presence of some source of background radiation which is less polarized than the collisionally redistributed signal. We have carried out investigations of how the polarization varies with probe laser detuning by scanning the laser

across line center. If we assume that the background is constant with small shifts from line center, then it is possible to arrive at an approximate value for the expected depression of polarization with the probe on line center, but taking into account its finite spectral width. At the working pressure of 2 Torr we have estimated this to be 3% (of measured value), not insignificant in comparison to the statistical error.

Scans of the probe laser frequency at different perturber pressures show that, as the pressure is increased, the profile of the signal scan broadens while the corresponding quantity for polarization narrows. This points towards the effect being collisional in origin, presumably collisional redistribution on the upper transition. Therefore, we can reasonably expect that the effect will not be present in our corrected data, which are extrapolated to zero pressure (see Sec. III B).

III. SECONDARY DEPOLARIZING MECHANISMS

There are a number of processes occurring after the initial collision that can reduce the alignment created in the excited state by the collisionally assisted excitation. These secondary depolarizing mechanisms are unrelated to the process of collisional redistribution in which we are interested. Corrections to the measured polarization must therefore be made in order to account for the effect of each of these secondary processes. We have previously discussed these corrections as applied to a single-step collisional redistribution experiment in Hg-Kr [7]. In the current experiment, however, the corrections necessitated by the depolarizing mechanisms generally differ to those for the single-step case. We therefore reexamine below the four secondary depolarizing mechanisms in relation to this experiment.

A. Depolarization due to hyperfine structure

The atom leaves the collisionally assisted excitation with populations $\rho_{M_J M_J}$ in the M_J states. These populations give the polarization in which we are interested through Eq. (2). If hyperfine structure has sufficient time to develop, then these populations will be distributed amongst the hyperfine states according to the tensor coupling relations. Where hyperfine structure is present ($I \neq 0$) this results in the fluorescence being significantly less polarized than would otherwise be the case. One may visualize this depolarization as being a result of the precession of the electronic angular momentum J, about the total angular momentum F, noting that the orientation of the nuclear spin I in space is random.

The collision duration may be estimated from $\tau_c = (\sigma_R / \pi \bar{v}^2)^{1/2}$, where σ_R is the "optical" cross section and $\bar{v}$ is the mean relative velocity between the colliding atoms. This leads to a value of 3 ps for $Hg(6\,^1S_0 - 6\,^3P_1) - Kr$ collisions, where $\sigma_R = (227 \pm 10) \times 10^{-20}$ m^2 [24]. The mercury hyperfine structure (of order 0.1 cm^{-1}) develops in a time $1/\Delta\omega_{\rm hfs} \sim 50$ ps. To a good approximation this occurs after the collision is complete and well before the probe laser pulse arrives. The collisional and hyperfine depolarizations may therefore be treated as separate and completed events.

Due to the short time scale over which the depolarization occurs, the effect of hyperfine structure in the present experiment is the same as in the single-step Hg-Kr experiment. The polarization P, corrected for the effect of hyperfine structure, is given by [7]

$$P = P_{\rm hfs}\left[1 - \left[\frac{2n^{1/2}}{9} + \frac{113n^{3/2}}{450}\right](3 - P_{\rm hfs})\right]^{-1} . \quad (4)$$

Here $P_{\rm hfs}$ is the polarization measured after the development of the hyperfine structure and n^I is the proportion of isotope with nuclear spin I in naturally occurring mercury ($n^{1/2} = 0.17, n^{3/2} = 0.13$). Equation (4) therefore provides a systematic prescription for converting the measured polarization into those which would be measured if there was no hyperfine structure (pure $I = 0$ mercury isotope).

B. Depolarization due to second collisions

The mean time between collisions is 21 ns with 2 Torr of Kr in the cell. Again this is estimated from the value of σ_R quoted above, using $T_c = (n_p \bar{v} \sigma_R)^{-1}$, where n_p is the perturber number density. It is therefore evident that a good proportion of $Hg(6\,^3P_1)$ atoms will suffer second collisions before the arrival of the probe laser pulse. As a result, the polarization of the fluorescence measured at time t_d will be lower than that which would be observed immediately after the collision.

The mercury atom leaves the collision in which excitation occurs with an alignment given by $\alpha^{(2)}$, the atomic alignment parameter. This quantity is proportional to the zeroth component of the quadrupolar alignment tensor $A_0^{(2)}$ [25], with the constant of proportionality being -1 in the $J = 1$ case. It is related to P, the polarization of fluorescence, through

$$\alpha^{(2)} = \frac{2P}{3 - P} . \quad (5)$$

This alignment is reduced to $\alpha_{\rm hfs}^{(2)}$ on a picosecond time scale as a result of the development of hyperfine structure in the $I \neq 0$ isotopes. This remaining alignment is further reduced before excitation by the probe laser pulse occurs through subsequent collisions with perturber atoms. It can be shown [26] that the alignment decays exponentially as a result of these collisions. The time constant $\gamma_c^{(2)}$ is given by

$$\gamma_c^{(2)} = n_p \langle v \sigma^{(2)} \rangle_{\rm av} , \quad (6)$$

where $\sigma^{(2)}$ is the cross section for alignment-destroying collisions.

If we can consider that the lasers have negligible pulse widths (see below), then the alignment measured is simply the alignment after a time t_d, the laser delay, has elapsed:

$$\alpha^{(2)}(t_d) = \alpha_{\rm hfs} e^{-\gamma_c^{(2)} t_d} . \quad (7)$$

Clearly this is a function of perturber density n_p. While it is desirable to keep secondary depolarization to a minimum by working at low pressure, this would also re-

sult in less signal and greater statistical error. All the detuning data presented here were taken with 2 Torr of Kr in the experimental cell. Under these conditions second collisions reduce the alignment measured at t_d to about 70% of its initial value.

By varying the krypton pressure at a fixed detuning it is possible to use Eq. (7) to calculate a value of $\gamma_c^{(2)} t_d$ at the working pressure (see Fig. 4). This may then be used to correct the detuning data without making assumptions as to the value of t_d or $\langle v\sigma^{(2)} \rangle_{\text{av}}$.

Using Eq. (5) it is possible to express the decay in alignment due to second collisions as a depolarization. The polarization which would be measured in the absence of second collisions P_{hfs} may then be expressed in terms of $P_{\text{sc}}(t_d)$, the polarization measured at the working pressure. We obtain

$$P_{\text{hfs}} = \frac{3P_{\text{sc}}(t_d)}{3e^{-\gamma_c^{(2)} t_d} - (1 - e^{-\gamma_c^{(2)} t_d}) P_{\text{sc}}(t_d)} . \tag{8}$$

The validity of the assumption that the laser pulse widths are negligible is certainly questionable given that the actual full widths at half maximum of 5 ns are significant compared to the delay (4 m). If we assume that the pulses are Gaussian, then the previously linear relationship between $\ln\alpha^{(2)}$ and pressure now becomes quadratic. In the pressure range of Fig. 4 the quadratic term remains rather small and no quadratic variation is evident in the plot. However, it is expected to lead to a systematic in the determination of gradient, which we estimate to be about 3% (comparable to the fitting error).

C. Depolarization due to the Hanle effect

The third source of depolarization is the Hanle effect due to the magnetic field of the Earth. This is analogous to the depolarization as a result of hyperfine structure, except that the field concerned is due to an external rather than an internal source. We can estimate the time scale for the depolarization caused by this process from the Larmor frequency in a field of 0.5 G. This gives a characteristic time of around 150 ns.

It can be shown that the Hanle effect results in a 7% depolarization for an initially 100% polarized state averaged over a 250-ns gate length [7]. The explanation for this small depolarization comes from the variation of the alignment as a function of time which is initially slow, becoming more pronounced at later times. Since we probe the excited-state alignment shortly after excitation then we should expect much less depolarization than this.

We have performed a calculation of the expected depolarization of the fluorescence 15 ns after excitation, with magnetic field direction and magnitude as appropriate to our experimental situation. In detail the calculation is very similar to that referred to above. We find that for an initially 100% polarized sample a depolarization of less than 0.1% would be expected. This is much smaller than the statistical error in the data and we disregard it in the following analysis.

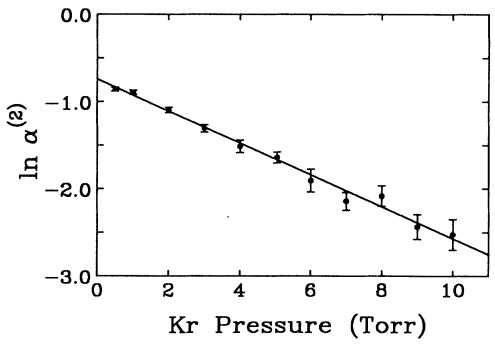

FIG. 4. Natural logarithm of atomic alignment parameter vs pressure of Kr in the experimental cell. The data shown are for a detuning of $-5\ \text{cm}^{-1}$. The exponential variation of alignment with perturber pressure due to second collisions is evident. Obtaining the gradient of the plot allows the detuning data to be corrected for the effect of second collisions.

D. Depolarization due to radiation trapping

Radiation trapping may also cause depolarization of the fluorescence. In a single-step experiment this occurs simply due to the fluorescent photons reexciting other Hg($6\,^1S_0$) atoms in the vapor surrounding the interaction region. In general, the excitation axis for the second atom will not coincide with that for the first. This results in the secondary radiation from the trapping atoms being less polarized than the fluorescence from the atoms excited directly by laser light.

In the current experiment, mercury atoms excited outside the second laser-beam path by reradiated photons will not lead to signal. Thus the effective trapping volume can be made much smaller than in a conventional experiment. We estimate a trapping length of 550 μm for mercury vapor pressure at room temperature (1.3×10^{-3} mbar). Assuming that each photon has an average distance of half the beam waist to travel before escaping the interaction region, then approximately 10% of all radiated photons will be trapped. A second factor that serves to reduce the influence of radiation trapping in this experiment is the fact that on arrival of the probe laser pulse only about 12% of the atoms have decayed. We therefore estimate that on arrival of the probe laser pulse just over 1% of the Hg($6\,^3P_1$) population will be due to secondary excitation. Since even these atoms will retain a considerable portion of the alignment of those initially excited by the first laser, then we expect the depolarization due to trapping to be somewhat below this level.

Clearly this estimation is the result of a very simple argument and we therefore chose to investigate the depolarization due to radiation trapping experimentally. To do this the cell was heated and the variation of polarization with signal level (as a measure of mercury vapor pressure) was monitored. We found no evidence of depolarization due to radiation trapping up to temperatures of around 50 °C, corresponding to a sevenfold increase in mercury vapor pressure. We are therefore confident that any effect at room temperature will be well inside the level of our statistical error and may safely be neglected.

In the single-step experiment radiation trapping was a

significant source of depolarization. Correction of the measured polarizations for radiation trapping was not very satisfactory and produced the dominant source of uncertaintly in the near wing polarization data. The removal of this effect is a major advantage of the present experiment.

E. Correction of measured polarizations

Our analysis above shows that hyperfine structure and second collisions are the only sources of secondary depolarization relevant to this experiment. Due to the vastly different time scales over which these processes occur, the corrections implied by Eq. (4) and (8) may be applied successively to the measured polarizations. They are applied in reverse order to that in which the processes occur, i.e., Eq. (8) is first applied, followed by Eq. (4).

The effect of applying the corrections at the highest measured polarizations of 47% leads to a corrected polarization of 73%. This should be compared to the single-photon experiment where a corrected polarization of this level would have been measured at 20%. The difference is largely due to the decreased influence of second collisions, but the absence of radiation trapping also plays a part. The higher measured polarizations tend to reduce any uncertainty arising from the correction process.

IV. RESULTS AND DISCUSSION

The variation of polarization with detuning for Hg-Kr collisional redistribution is shown in Fig. 5. All data points are corrected for secondary depolarizing mechanisms as set out in Sec. III.

The error bars shown in Fig. 5 represent the effect of statistical error on the measured polarizations, together with errors arising from the finite pressure correction (including the estimated systematic). Statistical error dominates at all detunings greater than about 10 cm^{-1}. Inside this detuning the error arising from the finite pressure correction becomes comparable to, and at the smallest detunings greater than, the statistical error. The signal falls off very rapidly in the red wing, which is reflected in high error bars at larger detunings. In contrast, the blue-wing signal holds up quite well in the region 20–150 cm^{-1}. This is due to the presence of satellites in the blue wing, which has been discussed by Findeisen and Grycuk [18].

No attempt has been made to correct the data for the systematics discussed above. On the basis of the estimates given we expect the combined effect of radiation trapping, the Hanle effect, and imperfect polarization of the lasers to be insignificant in comparison to the error bars shown.

Also plotted in Fig. 5 are the predictions of the simple quasiclassical model described in the Introduction. We use the interatomic potentials of Grycuk and co-workers [17,18] in this calculation. The result for polarization due to Lewis *et al.* [16] is employed, with decoupling radius R_{dc} determined by the Grosser [27] criterion,

$$\Delta V_{AB}(R_{dc}) = \frac{\hbar v_\infty}{R_{dc}} . \tag{9}$$

Here $\Delta V_{AB}(R)$ is the difference between the excited-state potentials and v_∞ is the asymptotic relative velocity in the upper state. At zero detuning this gives $R_{dc} \simeq 9.0$ Å for the above potentials (the variation with detuning is slight). In fact, Eq. (9) leads to multiple definitions of the decoupling radius, of which we take the outermost. The calculation is performed for a single-collision energy corresponding to 293 K, the temperature at which the experiment was performed.

In the near red wing excitation to the $B\,^3 1^{\pm}$ state is dominant and high polarizations characteristic of $1^{\pm}$ excitation are obtained. There is a discontinuous jump to

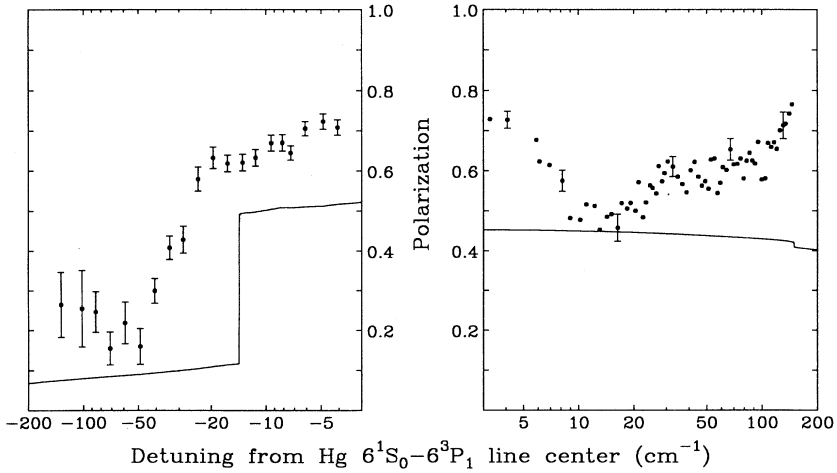

FIG. 5. Corrected detuning data. For clarity, error bars are only shown with every doubling of detuning in the blue wing. The solid line shows the predictions of a basic quasiclassical model embodying the assumptions set out in the Introduction. Calculational details are given in the text.

low polarizations after the red-wing satellite as here the model only allows excitation to the $A\,^3 0^+$ state. The blue-wing polarization remains high throughout the range as only the $B\,^3 1^\pm$ state may be accessed. The polarization falls off gradually in both wings as the Condon points move to lower interatomic separations, giving greater rotation of the molecular orbitals. In the far blue wing at around 150 cm^{-1} there is quite a sharp fall in the polarization due to this effect, as a local maximum in the difference potential is passed.

The quantitative predictions of this simple model are not in agreement with the data at almost all detunings. However, the main qualitative feature, the red-wing polarization switch is clearly borne out by the data. Reasons for the lack of quantitative agreement are not difficult to find. First, there is the purely classical effect of deviations from straight-line trajectories. At large detunings the Condon points move to small internuclear separations, increasing the average deflection angle and making bent trajectory effects important. Bent trajectories lead to higher polarizations since the rotation angles of the molecular orbitals are reduced [16]. The model predictions in the far wings are therefore expected to be unrealistically low due to the assumption of straight-line trajectories.

Second, there is the classical treatment of the red-wing satellite. In reality the absorption probability to the $B\,^3 1^\pm$ state does not drop to zero as soon as the difference potential minimum is passed. In fact, on the basis of a semiclassical treatment [28], it is expected to fall exponentially with detuning past the satellite. The polarization therefore continues to be influenced by the $B\,^3 1^\pm$ state on the dark side of the satellite, and will fall with the absorption probability to this state as the detuning is increased. Extensions to the basic quasiclassical model which remove this classical discontinuity have been proposed by Bieniek and co-workers [29,30].

The considerable underestimate of the polarization in the near wings is less easy to explain within the framework of the model. Definitions of the decoupling radius contain a certain amount of freedom and to some extent R_{dc} may be treated as an adjustable parameter. Pushing the decoupling radius to smaller values will increase the polarization due to reduced rotation of the orbitals. At small detunings there will be a further effect as the Condon radius becomes greater than the decoupling radius, and direct excitation to atomic, rather than molecular, states occurs. Excitation of the outgoing collision must in this case be assumed to lead to unity polarization, while a much lower value is obtained for excitation just inside the decoupling radius. This discontinuity can be removed if coherence between the different excited states is included in the model, which would also serve to push up polarizations in the near wing region [31].

Considerably more data were taken in the blue wing than in the red wing. The purpose of this was to attempt to reveal oscillatory structure that appears to be predicted by quantum-mechanical calculations [21]. This has been only partially successful as any oscillations in the far wing are apparently quite small, and at least partly masked by the statistical error in the data. A comparison of the results of coupled-channel calculations to the data should be a rather sensitive test of the interatomic potentials. We plan to undertake a full comparison and deal with questions arising from it in a later article [32].

V. CONCLUSIONS

We have developed a technique for monitoring the asymptotic alignment of mercury atoms following $Hg(6\,^1S_0-6\,^3P_1)-Kr$ collisional redistribution which avoids several of the problems associated with the single-step fluorescence-monitored experiment on this system. Greater signal allows us to cover the entire range of interesting detunings, while fewer uncertainties in the data correction process yields reduced error bars. We have therefore been able to draw some firm conclusions about the basic quasiclassical model. There is good agreement with the near red-wing data and the two blue-wing data points, which were taken using the single-step method [7].

An obvious extension of this work is to perform measurements in other rare-gas (RG) systems so that trends in the polarization spectrum with perturber mass and polarizability may be studied. Such work is at present underway in this laboratory. A more exciting prospect perhaps is the use of this system to study alignment effects following photodissociation of Hg-RG van der Waals complexes formed in a supersonic expansion. By virtue of Franck-Condon factors, excitation occurs to a specific electronic final state (the $B\,^3 1^\pm$ state) at a particular internuclear separation. A far more restricted range of angular momenta and kinetic energies than exist in the thermal cell experiments are involved in the subsequent "half-collision." It should therefore be possible to study directly the kinetic-energy dependence of the asymptotic alignment. We may also be able to study angular momentum dependence by altering the expansion conditions. Using a fully-quantum-mechanical time propagation method, Chen *et al.* [33,34] have recently performed calculations for the asymptotic alignment following photodissociation of Hg-Ar and Hg-Kr systems. In our planned experiment we aim to test these calculations and semiclassical models of the process based upon the decoupling radius concept.

We have already performed preliminary investigations of the asymptotic alignment following photodissociation, in an experiment where the polarization of the fluorescence on the Hg $6\,^1S_0-6\,^3P_1$ transition was monitored. The values of polarization obtained indicate that secondary depolarization mechanisms are certainly important in this arrangement. We believe that the most likely cause of this secondary depolarization is radiation trapping: although the mercury vapor densities will be low, due to continual pumping of the experimental chamber, the path length to detection is very long. We can expect the technique of the present experiment to eliminate this problem. Its application to the photodissociation case may therefore be essential in interpreting the results of such an experiment.

ACKNOWLEDGMENTS

We would like to thank F. Rebentrost and R. J. Bieniek for helpful discussions. Our thanks also go to G. R. K. Quelch for his help with the experiment. We gratefully acknowledge the financial support of the UK Science and Engineering Research Council.

[1] V. Kroop and W. Behmenburg, Z. Phys. A **294**, 299 (1980).
[2] P. Thomann, K. Burnett, and J. Cooper, Phys. Rev. Lett. **45**, 1325 (1980).
[3] W. J. Alford, K. Burnett, and J. Cooper, Phys. Rev. A **27**, 1310 (1983).
[4] W. J. Alford, N. Andersen, K. Burnett, and J. Cooper, Phys. Rev. A **30**, 2366 (1984).
[5] W. Behmenburg, V. Kroop, and F. Rebentrost, J. Phys. B **18**, 2693 (1985).
[6] W. J. Alford, N. Andersen, M. Belsley, J. Cooper, D. M. Warrington, and K. Burnett, Phys. Rev. A **31**, 3012 (1985).
[7] D. Segal and K. Burnett, J. Phys. B **22**, 247 (1989).
[8] D. Segal and I. D. Harris, J. Chem. Phys. **94**, 2713 (1991).
[9] K. Burnett and J. Cooper, Phys. Rev. A **22**, 2027 (1980); **22**, 2044 (1980).
[10] K. Burnett, J. Cooper, R. J. Ballagh, and E. W. Smith, Phys. Rev. A **22**, 2005 (1980).
[11] K. Burnett, Phys. Rep. **118**, 339 (1985).
[12] K. C. Kulander and F. Rebentrost, Phys. Rev. Lett. **51**, 1262 (1983).
[13] K. C. Kulander and F. Rebentrost, J. Chem. Phys. **80**, 5623 (1984).
[14] P. S. Julienne and F. H. Mies, Phys. Rev. A **30**, 831 (1984).
[15] P. S. Julienne and F. H. Mies, Phys. Rev. A **34**, 3792 (1986).
[16] E. L. Lewis, M. Harris, W. J. Alford, J. Cooper, and K. Burnett, J. Phys. B **16**, 553 (1983).
[17] T. Grycuk and E. Czerwosz, Physica C **106**, 431 (1981).
[18] M. Findeisen and T. Grycuk, J. Phys. B **22**, 1583 (1989).
[19] K. Fuke, T. Saito, and K. Kaya, J. Chem. Phys. **81**, 2591 (1984).
[20] M. Okunishi, H. Nakazawa, K. Yamanouchi, and S. Tsuchiya, J. Chem. Phys. **93**, 7526 (1990).
[21] F. Rebentrost (private communication).
[22] J. P. Barrat, J. L. Cojan, and Y. Lecluse, C. R. Acad. Sci. B **262**, 609 (1966).
[23] M. G. Littman and H. J. Metcalf, Appl. Opt. **14**, 2224 (1978).
[24] J. Butaux, F. Schuller, and R. Lennuier, J. Phys. (Paris) **35**, 361 (1974).
[25] U. Fano and J. H. Macek, Rev. Mod. Phys. **45**, 553 (1973).
[26] A. Omont, J. Phys. (Paris) **26**, 26 (1965).
[27] J. Grosser, J. Phys. B **14**, 1449 (1981).
[28] K. M. Sando and J. C. Wormhoudt, Phys. Rev. A **7**, 1889 (1973).
[29] R. J. Bieniek, Phys. Rev. A **35**, 3663 (1987).
[30] R. J. Bieniek, P. S. Julienne, and F. Rebentrost, J. Phys. B **24**, 5103 (1991).
[31] M. Glass-Maujean and J. A. Beswick, J. Chem. Soc. Faraday Trans. II **85**, 1031 (1989).
[32] F. Rebentrost, I. M. Bell, C. J. K. Quayle, and K. Burnett (unpublished).
[33] X. Chen, K. Burnett, and D. M. Segal, J. Chem. Phys. **95**, 8124 (1991).
[34] X. Chen and K. Burnett, J. Chem. Phys. **97**, 3175 (1992).